Remarks on boundary layers and matched asymptotics for an edge-buckling problem

(Supplementary online material)

Ciprian D. Coman[†], Andrew Bassom[‡]

1 Introduction

The following material revisits the interactive boundary-layer analysis presented in [2], offering additional insights into its applicability and limitations. It serves as a supplement to the main paper [1] (referred to as BC25 henceforth), and further motivates the results reported therein. Our aim is twofold. First, we confirm the consistency of the slightly unconventional asymptotic matching between the outer and inner solutions by systematically extending the previous analysis to higher orders. Second, we re-evaluate the relative accuracy of the resulting formula with respect to the various parameters appearing in the bifurcation equation. Our new findings indicate that the three-term asymptotic approximation derived in [2] (see Section 4 in that reference) is, in fact, optimal: for a fixed value of the asymptotic parameter, the inclusion of additional terms leads to a slight but consistent deterioration in predictive accuracy. Nevertheless, despite the overall high accuracy of the aforementioned result, certain limiting cases exhibit anomalous behaviour in the asymptotic formula, thereby prompting the further developments presented in BC25.

To ensure the present material is reasonably self-contained, we briefly re-iterate the main equations governing the linear bifurcation problem for the travelling web discussed in detail in [2] and summarised in BC25 as well. It is recalled the original boundary-value problem formulated in that work* corresponds to a simple ODE

$$\mathcal{L}[f] \equiv \beta^4 f'''' - 2\beta^2 f'' + (1 - \lambda + \eta y) f = 0\,, \qquad -1 < y < 1\,, \tag{1.1}$$

subject to the boundary conditions

$$\mathcal{B}_1[f] \equiv \beta^2 f'' - \nu f = 0\,, \qquad \mathcal{B}_2[f] \equiv \beta^2 f''' - (2-\nu) f' = 0\,, \qquad y = \pm 1\,, \tag{1.2}$$

where the 'dash' denotes differentiation with respect to y; $\lambda \in \mathbb{R}$ plays the role of eigenvalue (non-dimensional loading parameter), while $\eta = \mathcal{O}(1)$ (as $\beta \to 0^+$) is a given positive constant. The ordinary differential equation (1.1) arises from a separation-of-variables procedure applied to the original buckling PDE, with 'y' being the in-plane non-dimensional coordinate transverse to the axial (moving) direction of the web. The geometry of the web is assumed to be rectangular, with width

[†] cdc3p@yahoo.com

[‡] andrew.bassom@utas.edu.au

*The notation used here differs slightly from that adopted in [2]; in particular, the correspondence between the new and the old quantities is $\eta \to \widetilde{\alpha}$; see also §2 in [3], which contains additional details.

significantly exceeding length (see [2, 3] for full details). The *artificial* perturbation parameter $\beta > 0$ emerges as a by-product of the dimensional reduction and typically takes values of order $\mathcal{O}(10^{-2})$.

It is convenient to further re-scale the problem by introducing the new independent variable $\rho := 1 + \eta y$, which transforms (1.1)-(1.2) into a more tractable form

$$\delta^4 \frac{d^4 \widehat{f}}{d\rho^4} - 2\delta^2 \frac{d^2 \widehat{f}}{d\rho^2} + (\rho - \lambda)\widehat{f} = 0\,, \qquad \rho_- < \rho < \rho_+\,, \tag{1.3a}$$

$$\delta^2 \frac{d^2 \widehat{f}}{d\rho^2} - \nu \widehat{f} = 0\,, \qquad \rho = \rho_\pm\,, \tag{1.3b}$$

$$\delta^2 \frac{d^3 \widehat{f}}{d\rho^3} - (2 - \nu)\frac{d\widehat{f}}{d\rho} = 0\,, \qquad \rho = \rho_\pm\,, \tag{1.3c}$$

with $\rho_\pm := 1 \pm \eta$ and the new perturbation parameter $\delta := \eta\beta$, assumed to satisfy $0 < \delta \ll 1$. The main goal vis-à-vis the boundary-value problem (1.3) is to characterise the asymptotic behaviour of the critical (i.e., smallest) eigenvalue $\lambda \equiv \lambda(\delta)$, under the assumptions outlined above. In reference [2] the corresponding asymptotic analysis appears in Section 4.

The updated analysis included in the remainder of this document is organised as follows. The next section outlines the structure of the primary boundary layer (i.e., the "outer solution"), which is governed by a hierarchy of second-order Airy-type equations. The eigenvalue $\lambda \in \mathbb{R}$ is expanded in powers of δ, following the same asymptotic structure as in [2], with the expansion coefficients entering in the governing equations. Except for the first two, these coefficients remain undetermined at this stage. Their values are subsequently fixed by enforcing asymptotic matching with a secondary boundary layer (i.e., the "inner solution") nested within the primary structure. The details of this matching process are presented in §1.2. Although the solutions within the secondary-layer are relatively straightforward, enforcing the boundary conditions (1.3b)-(1.3c) introduces a non-trivial level of complexity. A numerical evaluation of the augmented earlier asymptotic approximation, together with a brief discussion of its implications, is provided in §1.3.

1.1 The main layer

The asymptotic structure of (1.3) relies on the interplay between two nested boundary-layers. In this section we deal with the larger structure, which has a characteristic size of order $\delta^{2/3}$ (see [2] for additional details). This suggests the introduction of a new rescaled variable $Y = \mathcal{O}(1)$ defined according to

$$\rho = \rho_- + \delta^{2/3} Y\,. \tag{1.4}$$

With this choice of independent variable, solutions of the bifurcation problem (1.3) will be sought with an ansatz of the form

$$\widehat{f} = \sum_{j=0}^{\infty} F_j(Y)\,\delta^{j/3} \qquad \text{and} \qquad \lambda = \sum_{j=0}^{\infty} \lambda_j\,\delta^{j/3}\,, \tag{1.5}$$

in which the functions $F_j \equiv F_j(Y)$ and the coefficients λ_j $(j = 0, 1, 2, \dots)$ are to be found by substituting (1.5) in (1.3), followed by the usual manipulations. At leading- and next-to-leading orders this process results in an algebraic relation

$$\lambda_0 = \rho_- \equiv 1 - \eta\,, \tag{1.6}$$

together with the requirement that $\lambda_1 = 0$. In order for the second ansatz in (1.5) to qualify as an asymptotic expansion, it is necessary to impose the additional condition $0 < 1-\eta = \mathcal{O}(1)$ (as $\delta \to 0^+$); essentially, $|\lambda_0|$ must be asymptotically larger than the magnitude of the first non-zero correction term in that expansion.

The next information that transpires is just a re-scaled homogeneous Airy equation,

$$2\frac{d^2F_0}{dY^2} - (Y-\lambda_2)F_0 = 0\,;$$

this is easily handled by introducing the change of variable

$$Z := \frac{1}{\sqrt[3]{2}}\big(Y-\lambda_2\big)\,, \tag{1.7}$$

which immediately shows that $\widehat{F}_0(Z) \equiv F_0(Y(Z)) = \mathrm{Ai}(Z)$, where 'Ai' denotes the usual Airy function that decays exponentially quickly as $Z \to +\infty$. Without loss of generality, the (arbitrary) proportionality constant in this solution has been chosen to be unity.

It is readily seen that F_0 cannot satisfy both boundary conditions (1.3b) and (1.3c) at $Y = 0$. When these constraints are expressed in terms of the BL variable Y, one finds that either F_0 or its first derivative must vanish at $Y = 0$, but not both. This ambiguity is typically resolved by examining the solution structure of the original ODE (1.3a) within an additional, thinner boundary-layer localised near $Y = 0$; a comparable (though unrelated) analysis can be found in [4]. This issue is addressed in greater detail in BC25, where it is explained that neither choice alone reproduces the correct mathematical structure of the *critical* eigenmode for the buckling problem (1.3). A more pragmatic approach was pursued in [2], based on direct numerical simulations, which suggested that enforcing the condition $dF_0/dY = 0$ at $Y = 0$ yields a fairly robust approximation of λ, even for moderate values of δ (provided that $\nu \simeq 0.3$ or smaller). The trade-off for this simplification is a somewhat unorthodox handling of the additional boundary-layer mentioned above, the implications of which are clarified in §1.2. For now, we follow [2] and impose $d\widehat{F}_0/dZ = 0$ at $Y = 0$, which leads to

$$\lambda_2 = \sqrt[3]{2}\zeta_{01}\,, \tag{1.8}$$

where $(-\zeta_{01}) \simeq -1.0188$ is the first zero of the *derivative* of the Airy function of the first kind, i.e. $\mathrm{Ai}^{(1)}(-\zeta_{01}) = 0$. Throughout the following discussion, superscripts on functions of Z denote derivatives with respect to that variable.

Subsequently, we find a hierarchy of variable-coefficient differential equations

$$2\frac{d^2F_j}{dY^2} - (Y-\lambda_2)F_j = -\sum_{k=0}^{j-1}\lambda_{j+2-k}F_k + \frac{d^4F_{j-2}}{dY^4}\,, \qquad j \geq 1\,, \tag{1.9}$$

where we have adopted the convention $F_{-1} \equiv 0$.

The determination of λ_j ($j = 2, 3, \dots$) in the proposed approximation for the eigenparameter – see (1.5), can be carried out systematically by solving the sequence of equations in (1.9) subject to asymptotic matching with the solution developed later in §1.2.

The governing equation for $F_1(Y)$ is obtained by taking $j = 1$ in (1.9). With the help of the transformation (1.7) this can be cast as a standard inhomogeneous Airy equation; a particular solution $\widehat{F}_1(Z) \equiv F_1(Y(Z))$ consistent with the localised behaviour we are interested in is given by

$$\widehat{F}_1(Z) = \gamma\mathrm{Ai}^{(1)}(Z)\,, \qquad \text{with} \quad \gamma := -\frac{\lambda_3}{\sqrt[3]{2}}\,. \tag{1.10}$$

The function $F_2(Y)$ in (1.5) is similarly identified by considering the equation (1.9) for $j = 2$. Following the same strategy as above, it can be shown that a particular solution $\widehat{F}_2(Z) \equiv F_2(Y(Z))$ is

$$\widehat{F}_2(Z) = a_1 \mathrm{Ai}^{(1)}(Z) + a_2 \mathrm{Ai}^{(2)}(Z) + a_3 \mathrm{Ai}^{(5)}(Z)\,, \tag{1.11}$$

where

$$a_1 := -\frac{\lambda_4}{\sqrt[3]{2}}\,, \qquad a_2 := \frac{\lambda_3^2}{2\sqrt[3]{4}}\,, \qquad a_3 := \frac{1}{10\sqrt[3]{4}}\,.$$

The process illustrated above can be continued indefinitely. However, for our immediate purposes we will need only $F_3(Y)$ and $F_4(Y)$; the governing equation for the former function is found by setting $j = 3$ in (1.9). Using the change of variable (1.7), after some routine manipulations, we discover that $\widehat{F}_3(Z) \equiv F_3(Y(Z))$ can be expressed as

$$\widehat{F}_3(Z) = b_1 \mathrm{Ai}^{(1)}(Z) + b_2 \mathrm{Ai}^{(2)}(Z) + b_3 \mathrm{Ai}^{(3)}(Z) + b_4 \mathrm{Ai}^{(6)}(Z)\,, \tag{1.12}$$

where

$$b_1 := -\frac{\lambda_5}{\sqrt[3]{2}}\,, \qquad b_2 := \frac{\lambda_3\lambda_4}{\sqrt[3]{4}}\,, \qquad b_3 := -\frac{\lambda_3^3}{12}\,, \qquad b_4 := -\frac{\lambda_3}{20}\,.$$

Finally, the differential equation for $F_4(Y)$ corresponds to $j = 4$ in (1.9). Once more, with the use of the change of variable (1.7), we find that $\widehat{F}_4(Z) \equiv F_4(Y(Z))$ admits the expression

$$\widehat{F}_4(Z) = d_1 \mathrm{Ai}^{(1)}(Z) + d_2 \mathrm{Ai}^{(2)}(Z) + d_3 \mathrm{Ai}^{(3)}(Z) + d_4 \mathrm{Ai}^{(4)}(Z) + d_5 \mathrm{Ai}^{(6)}(Z) + d_6 \mathrm{Ai}^{(7)}(Z) + d_7 \mathrm{Ai}^{(10)}(Z)\,, \tag{1.13}$$

where

$$d_1 := -\frac{\lambda_6}{\sqrt[3]{2}}\,, \qquad d_5 := -\frac{\lambda_4}{20}\,, \tag{1.14a}$$

$$d_2 := \frac{1}{2\sqrt[3]{4}}\left(\lambda_4^2 + 2\lambda_3\lambda_5\right)\,, \qquad d_6 := \frac{\lambda_3^2}{40\sqrt[3]{2}}\,, \tag{1.14b}$$

$$d_3 := -\frac{\lambda_3^2\lambda_4}{4}\,, \qquad d_7 := \frac{1}{400\sqrt[3]{2}}\,, \tag{1.14c}$$

$$d_4 := \frac{\lambda_3^4}{48\sqrt[3]{2}}\,. \tag{1.14d}$$

Before moving on to the next section, some remarks are in order. As explained in [11], the differential equation (1.3a) admits another distinguished limit, which corresponds to a nested (bending) boundary layer. Intuitively, for $0 < \delta \ll 1$ strong bending effects are primarily localised within a narrow layer of characteristic size $\mathcal{O}(\delta)$ adjacent to $\rho = \rho_-$. The systematic description of these effects requires introducing the new re-scaled variable $\overline{Y} = \mathcal{O}(1)$ defined by

$$\rho = \rho_- + \delta\,\overline{Y}\,. \tag{1.15}$$

To figure out the structure of the solution in the nested thin region we expand the main-layer solution in terms of the new variable $\overline{Y}$. Defining $\widehat{f}_{\mathrm{out}}$ as the solution $\widehat{f}$ in the ansatz (1.5), and noting that

$Y = \delta^{1/3}\,\overline{Y}$, we have

$$\widehat{f}_{\rm out} = \sum_{j=0}^{\infty} \left\{ \sum_{\substack{p+q=j \\ p,q\geq 0}} \left(\frac{\Pi_{pq}}{2^{q/3} q!} \right) \overline{Y}^q \right\} \delta^{j/3}\,, \tag{1.16}$$

where the constants $\Pi_{kj} \in \mathbb{R}$ are defined by

$$\Pi_{pq} := \begin{cases} \dfrac{d^q \widehat{F}_p}{dZ^q}\Big|_{Z=-\zeta_{01}} & \text{if} \quad q \geq 1\,, \\ \widehat{F}_p(-\zeta_{01}) & \text{if} \quad q = 0\,. \end{cases}$$

To make things a bit more transparent it is helpful to write out the first few terms in (1.16),

$$\begin{aligned} \widehat{f}_{\rm out} = \Pi_{00} + \left(\Pi_{10} + \frac{1}{\sqrt[3]{2}} \Pi_{01} \overline{Y} \right) \delta^{1/3} + \left(\Pi_{20} + \frac{1}{\sqrt[3]{2}} \Pi_{11} \overline{Y} + \frac{1}{2\sqrt[3]{4}} \Pi_{02} \overline{Y}^2 \right) \delta^{2/3} \\ + \left(\Pi_{30} + \frac{1}{\sqrt[3]{2}} \Pi_{21} \overline{Y} + \frac{1}{2\sqrt[3]{4}} \Pi_{12} \overline{Y}^2 + \frac{1}{12} \Pi_{03} \overline{Y}^3 \right) \delta \\ + \left(\Pi_{40} + \frac{1}{\sqrt[3]{2}} \Pi_{31} \overline{Y} + \frac{1}{2\sqrt[3]{4}} \Pi_{22} \overline{Y}^2 + \frac{1}{12} \Pi_{13} \overline{Y}^3 + \frac{1}{48\sqrt[3]{2}} \Pi_{04} \overline{Y}^4 \right) \delta^{4/3} + \dots\,. \end{aligned} \tag{1.17}$$

We note in passing that all the Π-coefficients written down in (1.17) can be calculated with the help of the expressions for $\widehat{F}_p$ ($p = 0, 1, \dots$) recorded above. In particular, the $\mathcal{O}(\delta^{1/3})$-part of $\widehat{f}_{\rm out}$ will drop out since $\Pi_{10} = \Pi_{01} = 0$. The expression of the other coefficients are recorded below for further reference

$$\Pi_{00} = {\rm Ai}(-\zeta_{01}) \equiv {\rm Ai}_0\,, \qquad \Pi_{02} = -\zeta_{01}{\rm Ai}_0\,, \qquad \Pi_{03} = {\rm Ai}_0\,, \qquad \Pi_{04} = \zeta_{01}^2 {\rm Ai}_0\,, \tag{1.18a}$$

$$\Pi_{11} = -\zeta_{01}\gamma{\rm Ai}_0\,, \qquad \Pi_{12} = \gamma{\rm Ai}_0\,, \qquad \Pi_{13} = \zeta_{01}^2\gamma{\rm Ai}_0\,, \tag{1.18b}$$

$$\Pi_{20} = -(a_2 + 4a_3)\zeta_{01}{\rm Ai}_0\,, \qquad \Pi_{21} = \big[(a_2 + 4a_3) - a_1\zeta_{01} - a_3\zeta_{01}^3\big]{\rm Ai}_0\,, \tag{1.18c}$$

$$\Pi_{22} = \big[a_1 + (a_2 + 9a_3)\zeta_{01}^2\big]{\rm Ai}_0\,, \qquad \Pi_{30} = \big[(b_3 + 4b_4) - b_2\zeta_{01} - b_4\zeta_{01}^3\big]{\rm Ai}_0\,, \tag{1.18d}$$

$$\Pi_{31} = \big[b_2 - b_1\zeta_{01} + (b_3 + 9b_4)\zeta_{01}^2\big]{\rm Ai}_0\,, \tag{1.18e}$$

$$\Pi_{40} = \big[(d_3 + 4d_5) - d_2\zeta_{01} + (d_4 + 9d_6 + 100d_7)\zeta_{01}^2 - d_5\zeta_{01}^3 - d_7\zeta_{01}^5\big]{\rm Ai}_0\,. \tag{1.18f}$$

1.2 The secondary layer & matching

Following [2] an approximation of the inner-layer solution will be sought with an ansatz of the form

$$f = \widehat{f}_{\rm inn} \equiv f_0(\overline{Y}) + \delta^{2/3} f_1(\overline{Y}) + \delta f_2(\overline{Y}) + \delta^{4/3} f_3(\overline{Y}) + \delta^{5/3} f_4(\overline{Y}) + \dots\,, \tag{1.19}$$

in which the functions f_j ($j = 0, 1, 2, \dots$) will be determined sequentially by solving a hierarchy of fourth-order differential problems; as $\overline{Y} \to +\infty$, it is also necessary for these solutions not to exhibit exponential growth. In the light of the comments made immediately after (1.17), the contribution corresponding to the $\delta^{1/3}$ term in (1.19) was left out.

The usual substitutions lead to the following sequence of order equations

$$\frac{d^4 f_j}{d\overline{Y}^4} - 2\frac{d^2 f_j}{d\overline{Y}^2} = \mathcal{R}_j\,, \qquad (j = 0, 1, 2, \dots)\,, \tag{1.20}$$

in which the first few right-hand sides $\mathcal{R}_j$ assume the following expressions

$$\mathcal{R}_0 \equiv 0\,, \qquad \mathcal{R}_1 \equiv \lambda_2 f_0\,, \qquad \mathcal{R}_2 \equiv -\left(\overline{Y} - \lambda_3\right) f_0\,, \qquad \mathcal{R}_3 \equiv \lambda_2 f_1 + \lambda_4 f_0\,, \dots\,. \tag{1.21}$$

The equations in (1.20) must be solved subject to the transformed version of the original constraints (1.3b)-(1.3c), namely

$$\frac{d^2 f_j}{d\overline{Y}^2} - \nu f_j = 0 \qquad \text{and} \qquad \frac{d^3 f_j}{d\overline{Y}^3} - (2-\nu)\frac{df_j}{d\overline{Y}} = 0 \qquad \text{at} \quad \overline{Y} = 0\,. \tag{1.22}$$

However, the solution of these boundary-value problems alone does not fully determine the functions f_j $(j = 0, 1, 2, \dots)$. To uniquely specify them, it is also necessary to incorporate the asymptotic matching conditions derived in the previous section, ensuring consistency between the contributions from both boundary layers.

The leading-order term in the expansion (1.19) is obtained by solving (1.20) with $j = 0$. Discarding the exponentially growing part of the general solution, the resulting expression is

$$f_0(\overline{Y}) = c_1 \mathrm{e}^{-\overline{Y}\sqrt{2}} + c_2 + c_3 \overline{Y}\,, \tag{1.23}$$

where $c_j \in \mathbb{R}$ $(j = 1, 2, 3)$. Attempting to impose both conditions in (1.22) with $j = 0$ on this function yields the result that c_1 and c_2 must be proportional to c_3. Subsequent matching with the $\mathcal{O}(1)$ part of the outer-inner expansion (1.17) then forces $c_3 = 0$, and consequently $c_1 = c_2 = 0$. That is, $f_0 \equiv 0$, which contradicts that we have chosen $\Pi_{00} \neq 0$. The inconsistency identified in the preceding analysis suggests that the appropriate boundary condition on the leading-order outer solution should be $F_0 = 0$ at $Y = 0$. This, in turn, implies that ζ_{01} in equation (1.8) should also be replaced by ζ_0, where $(-\zeta_0) \simeq -2.33811$ is the first zero of the Airy function, i.e. $\mathrm{Ai}(-\zeta_0) = 0$.

In the present context, an alternative approach may be used to reconcile expressions (1.23) and (1.17), albeit without fully enforcing the boundary constraints (1.22). To this end, recall that the leading-order outer solution F_0 was constructed to satisfy (1.3c); therefore, to maintain consistency, the leading-order inner solution must at least comply with the complementary boundary condition (1.3b). This constraint imposes a linear relationship between the constants c_1 and c_2, while leaving c_3 undetermined. However, asymptotic matching between (1.17) and (1.23) requires $c_3 = 0$, and the remaining two constants are uniquely identified as

$$c_1 = \frac{\nu \mathrm{Ai}_0}{2-\nu} \qquad \text{and} \qquad c_2 = \mathrm{Ai}_0\,. \tag{1.24}$$

The remaining terms in the inner-solution ansatz (1.19) are determined in a standard manner – by enforcing both boundary conditions in (1.22)), as explained earlier. Despite the unconventional strategy used to determine the first term f_0, the matching between the two distinct boundary-layer structures remains consistent and permits the sequential determination of the coefficients λ_j in (1.5), up to at least the sixth order. The limitations of this pragmatic approach will only become apparent in §1.3, where the relative accuracy of the asymptotic predictions for λ is assessed against direct numerical simulation of the buckling problem (1.3).

To find $f_1(\overline{Y})$ we must solve (1.20) with $j = 1$; this will require the expression (1.23). The general solution of this equation can be shown to be

$$f_1(\overline{Y}) = (c_4\overline{Y} + c_5)\,\mathrm{e}^{-\overline{Y}\sqrt{2}} - \frac{1}{4}\lambda_2\mathrm{Ai}_0\underline{\overline{Y}^2} + c_6 + c_7\overline{Y}\,, \tag{1.25}$$

where

$$c_4 := -\frac{\nu\lambda_2\mathrm{Ai}_0}{4\sqrt{2}(2-\nu)}\,, \qquad c_5 := \frac{c_8}{2} - \frac{5\nu\lambda_2\mathrm{Ai}_0}{16(2-\nu)}\,,$$

and the new constants c_6, c_7, $c_8 \in \mathbb{R}$ are determined as explained next.

Applying the boundary conditions (1.3b) and (1.3c) gives

$$c_8 := \frac{2\nu c_6}{2-\nu} + \frac{\lambda_2(16 - 6\nu - 5\nu^2)\mathrm{Ai}_0}{8(2-\nu)^2}\,, \qquad c_7 := -\frac{\nu^2\sqrt{2}c_6}{(2-\nu)^2} + \frac{\lambda_2\nu(\nu^2 + 10\nu - 16)\mathrm{Ai}_0}{4\sqrt{2}(2-\nu)^3}\,. \tag{1.26}$$

The first of these two constants (c_8) is inconsequential for our immediate purposes, but we remark that c_7 will have to match the linear part of the $\mathcal{O}(\delta^{2/3})$-term in the asymptotic result (1.17), i.e.

$$c_7 = \frac{\Pi_{11}}{\sqrt[3]{2}}\,.$$

An important observation at this juncture is that the quadratic term in that expansion is identical to the (underlined) one in (1.25), a fact that reinforces the consistency of our asymptotic expansions. Further noting that $c_6 = \Pi_{20}$, use of (1.26) and (1.18) in conjunction with the matching requirement mentioned above leads to a quadratic equation in λ_3,

$$5\nu^2(2-\nu)\lambda_3^2 - 5\sqrt{2}(2-\nu)^3\lambda_3 - \frac{1}{2}\nu(3\nu^2 - 66\nu + 80) = 0\,; \tag{1.27}$$

the solution of interest (i.e., the one smallest in absolute value) can be cast in explicit form. Equation (1.27) is equivalent to its counterpart in [2], specifically equation (4-22) in that work. This equivalence is not immediately apparent as the present analysis is based on the re-scaled formulation (1.3) rather than the original version (1.1) used previously. Given that ν is a *relatively* small parameter, the expression of λ_3 in (1.27) may be approximated by the asymptotic expansion

$$\lambda_3 \simeq -\frac{\nu}{10\sqrt{2}}\left(10 + \frac{27}{4}\nu^2 + 3\nu^3 - \frac{9}{10}\nu^4 - \frac{53}{16}\nu^5 - \frac{5949}{1280}\nu^6\right)\,, \tag{1.28}$$

which reproduces the exact value with a relative error of less than 0.5% across the full admissible range of Poisson's ratio. We also note that a numerical evaluation of (1.27) confirms that $\lambda_3 \equiv \lambda_3(\nu) < 0$ for all $0 < \nu < 0.5$, and that λ_3 is monotonically decreasing function of ν on this interval.

Next, we examine the solution of (1.20) for $j = 2$. This function admits the representation stated below

$$f_2(\overline{Y}) = (G_0 + G_1\overline{Y} + G_2\overline{Y}^2)\,\mathrm{e}^{-\overline{Y}\sqrt{2}} + G_3 + G_4\overline{Y} + G_5\overline{Y}^2 + G_6\overline{Y}^3\,, \tag{1.29}$$

where

$$G_0 := \frac{c_{11}}{2} + \frac{1}{16}\left(\frac{17}{2\sqrt{2}} - 5\lambda_3\right)c_1\,, \qquad G_4 := c_{10}\,, \tag{1.30a}$$

$$G_1 := \frac{1}{4}\left(\frac{5}{4} - \frac{\lambda_3}{\sqrt{2}}\right)c_1\,, \qquad G_5 := -\frac{1}{4}\lambda_3 c_2\,, \tag{1.30b}$$

$$G_2 := \frac{c_1}{8\sqrt{2}}\,, \qquad\qquad G_6 := \frac{c_2}{12}\,, \tag{1.30c}$$

$$G_3 := c_9\,; \tag{1.30d}$$

the newly introduced constants c_9, c_{10}, $c_{11} \in \mathbb{R}$ are determined from the boundary conditions and the matching with the outer solution. The former shows that

$$c_{11} = -\frac{2\nu c_9}{\nu-2} + \frac{\mathcal{P}_{11}}{(2-\nu)^2}\,, \qquad c_{10} = -\frac{\nu^2\sqrt{2}c_9}{(2-\nu)^2} + \frac{\mathcal{P}_{10}}{(2-\nu)^3}\,, \tag{1.31}$$

with

$$\mathcal{P}_{11} := \left[2\lambda_3 - \frac{\nu}{16}(\sqrt{2}+12\lambda_3) + \frac{\nu^2}{32}(17\sqrt{2}-20\lambda_3)\right]\mathrm{Ai}_0\,,$$

$$\mathcal{P}_{10} := \left[2 - \nu(1+2\sqrt{2}\lambda_3) - \frac{\nu^2}{8}(3-10\sqrt{2}\lambda_3) - \frac{\nu^3}{16}(5-2\sqrt{2}\lambda_3)\right]\mathrm{Ai}_0\,.$$

Matching the above expression of $f_2(\overline{Y})$ to the corresponding $\mathcal{O}(\delta)$ contributions in (1.17) yields

$$G_3 = \Pi_{30}\,, \qquad G_4 = \frac{\Pi_{21}}{\sqrt[3]{2}}\,, \qquad G_5 = \frac{\Pi_{12}}{2\sqrt[3]{4}}\,, \qquad G_6 = \frac{\Pi_{03}}{12}\,. \tag{1.32}$$

It is a routine matter to check that the last two are in fact identically satisfied, while the remaining relations provide a linear equation for determining λ_4,

$$-\frac{\nu^2\sqrt{2}\,\Pi_{30}}{(2-\nu)^2} + \frac{\mathcal{P}_{10}}{(2-\nu)^3} = \frac{\Pi_{21}}{\sqrt[3]{2}}\,. \tag{1.33}$$

Although there is no significant difficulty in providing an explicit formula for λ_4, the result is complicated and not particularly insightful. Once the coefficients of (1.33) are numerically evaluated, the solution can be found trivially. In particular, it can be checked numerically that $\lambda_4 \equiv \lambda_4(\nu) > 0$ for all $0 < \nu < 0.5$.

Moving on to the next order, the solution $f_3(\overline{Y})$ can be obtained from (1.20) for $j = 3$ by taking into consideration the expressions of f_0 and f_1 already derived above. The result can be cast in a form similar to (1.29), namely

$$f_3(\overline{Y}) = (H_0 + H_1\overline{Y} + H_2\overline{Y}^2)\,\mathrm{e}^{-\overline{Y}\sqrt{2}} + H_3 + H_4\overline{Y} + H_5\overline{Y}^2 + H_6\overline{Y}^3 + H_7\overline{Y}^4\,, \tag{1.34}$$

where

$$H_0 := \frac{c_{14}}{2} - \frac{1}{16}\left(\frac{17c_4}{2\sqrt{2}} + 5c_5\right)\lambda_2 - \frac{5\lambda_4 c_1}{16}\,, \qquad H_4 := c_{13}\,, \tag{1.35a}$$

$$H_1 := -\frac{1}{4}\left(\frac{5c_4}{4} + \frac{c_5}{\sqrt{2}}\right)\lambda_2 - \frac{\lambda_4 c_1}{4\sqrt{2}}\,, \qquad H_5 := \frac{1}{4}\left[\left(\frac{\lambda_2^2}{4} - \lambda_4\right)c_2 - \lambda_2 c_6\right]\,, \tag{1.35b}$$

$$H_2 := -\frac{\lambda_2 c_4}{8\sqrt{2}}\,, \qquad H_6 := -\frac{\lambda_2 c_7}{12}\,, \tag{1.35c}$$

$$H_3 := c_{12}\,, \qquad H_7 := \frac{\lambda_2^2 c_2}{96}\,. \tag{1.35d}$$

The constants c_{12}, c_{13}, $c_{14} \in \mathbb{R}$ are determined from the boundary conditions and the matching with the outer solution. Using (1.3b) and (1.3c) results in

$$c_{14} = -\frac{2\nu c_{12}}{\nu-2} + \frac{\mathcal{P}_{14}}{\nu-2} + \frac{\mathcal{Q}_{14}}{(\nu-2)^2}\,, \tag{1.36a}$$

$$c_{13} = -\frac{\nu^2\sqrt{2}c_{12}}{(\nu-2)^2} + \frac{\lambda_2 c_7}{2(\nu-2)} + \frac{\mathcal{P}_{13}}{(\nu-2)^2} + \frac{\mathcal{Q}_{13}}{(\nu-2)^3}\,, \tag{1.36b}$$

with

$$\mathcal{P}_{14} := \frac{1}{4}\lambda_2^2 \mathrm{Ai}_0 + \left[\frac{\sqrt{2}}{32}(17\nu-2)c_4 + \frac{5\nu c_5}{8} - \frac{1}{4}(c_5+4c_6)\right]\lambda_2\,,$$

$$\mathcal{Q}_{14} := -\frac{1}{8}(5\nu^2+6\nu-16)\lambda_4 \mathrm{Ai}_0\,,$$

$$\mathcal{P}_{13} := \frac{\sqrt{2}}{8}\nu\lambda_2^2\mathrm{Ai}_0 + \left\{\frac{1}{16}(5\nu^2+14\nu-16)c_4 + \frac{\sqrt{2}}{8}\left[(\nu^2+6\nu-8)c_5 - 4\nu c_6\right]\right\}\lambda_2\,,$$

$$\mathcal{Q}_{13} := -\frac{\nu\sqrt{2}}{8}(\nu^2+10\nu-16)\lambda_4\mathrm{Ai}_0\,.$$

To find λ_5 we need to examine the matching between (1.34) and the $\mathcal{O}(\delta^{4/3})$ contributions in (1.17); this results in the following relations

$$H_3 = \Pi_{40}\,, \qquad H_4 = \frac{\Pi_{31}}{\sqrt[3]{2}}\,, \qquad H_5 = \frac{\Pi_{22}}{2\sqrt[3]{4}}\,, \qquad H_6 = \frac{\Pi_{13}}{12}\,, \qquad H_7 = \frac{\Pi_{04}}{48\sqrt[3]{2}}\,. \tag{1.37}$$

With the help of the previous matching conditions and the information from (1.18), it is a simple exercise to check that the last three relations are automatically satisfied; the first two can be combined to yield a linear equation for λ_5,

$$-\frac{\nu^2\sqrt{2}\,\Pi_{40}}{(2-\nu)^2} + \frac{\lambda_2 c_7}{2(\nu-2)} + \frac{\mathcal{P}_{13}}{(2-\nu)^2} + \frac{\mathcal{Q}_{13}}{(\nu-2)^3} = \frac{\Pi_{31}}{\sqrt[3]{2}}\,. \tag{1.38}$$

It is found numerically that $\lambda_5 \equiv \lambda_5(\nu) < 0$ for all $0 < \nu < 0.5$, but the size of the term $\lambda_5\delta^{5/3}$ is not big enough to compensate for the fact that the preceding contribution in the expansion of λ was positive. In other words, the newly calculated terms corresponding to λ_j ($j = 4, 5$) do not enhance the accuracy of the result previously derived in [2]. In the interest of completeness, it would be desirable to calculate the next-order coefficient λ_6; only the key results needed in deriving the relevant linear equation for determining this quantity will be included below.

First, we require an extra contribution to the outer solution. This corresponds to the function $F_5(Y)$ in the ansatz (1.5), and whose governing equation is given by (1.9) with $j = 5$. Its solution can be cast in the form

$$\widehat{F}_5(Z) = \sum_{j=0}^{10} \frac{\beta_j}{j+1}\mathrm{Ai}^{(j+1)}(Z)\,, \tag{1.39}$$

where

$$\beta_0 := -\frac{\lambda_7}{\sqrt[3]{2}}\,, \qquad\qquad \beta_6 := -\frac{1}{\sqrt[3]{2}}(b_4\lambda_4 + d_5\lambda_3) + \frac{b_2}{2\sqrt[3]{4}}\,,$$

$$\beta_1 := -\frac{1}{\sqrt[3]{2}}(\gamma\lambda_6 + a_1\lambda_5 + b_1\lambda_4 + d_1\lambda_3)\,, \qquad \beta_7 := -\frac{d_6\lambda_3}{\sqrt[3]{2}} + \frac{b_3}{2\sqrt[3]{4}}\,,$$

$$\beta_2 := -\frac{1}{\sqrt[3]{2}}(a_2\lambda_5 + b_2\lambda_4 + d_2\lambda_3)\,, \qquad \beta_8 \equiv \beta_9 := 0\,,$$

$$\beta_3 := -\frac{1}{\sqrt[3]{2}}(b_3\lambda_4 + d_3\lambda_3)\,, \qquad \beta_{10} := -\frac{d_7\lambda_3}{\sqrt[3]{2}} + \frac{b_4}{2\sqrt[3]{4}}\,,$$

$$\beta_4 := -\frac{d_4\lambda_3}{\sqrt[3]{2}}\,, \qquad \beta_5 := -\frac{a_3\lambda_5}{\sqrt[3]{2}} + \frac{b_1}{2\sqrt[3]{4}}\,.$$

With this information in hand, it then follows that

$$\Pi_{50} = \frac{1}{3}(\beta_2 + 2\beta_5) - \left(\frac{\beta_1}{2} + \frac{4\beta_4}{5} + \frac{7\beta_7}{2} + \frac{280}{11}\beta_{10}\right)\zeta_{01} + \left(\frac{\beta_3}{4} + \frac{9\beta_6}{7}\right)\zeta_{01}^2 - \frac{1}{6}\beta_5\zeta_{01}^3 + \left(\frac{\beta_7}{8} + \frac{25}{11}\beta_{10}\right)\zeta_{01}^4\,, \quad (1.40)$$

while the previously calculated $\widehat{F}_4(Z)$ yields

$$\Pi_{41} = d_2 - \big[d_1 + 4(d_4 + 7d_6 + 70d_7)\big]\zeta_{01} + (d_3 + 9d_5)\zeta_{01}^2 + (d_6 + 25d_7)\zeta_{01}^4\,. \quad (1.41)$$

In addition to the new information recorded above, the expression of the inner solution $f_4(\overline{Y})$ must also be identified. To this end, we note that the corresponding right-hand side in (1.20) assumes the expression

$$\mathcal{R}_4 \equiv \lambda_2 f_2(\overline{Y}) + \lambda_5 f_0(\overline{Y}) - (Y - \lambda_3) f_1(\overline{Y})\,.$$

Routine (but lengthy) calculations show that the solution of interest is

$$f_4(\overline{Y}) = \left(\sum_{j=0}^{3} K_j \overline{Y}^j\right) \mathrm{e}^{-\overline{Y}\sqrt{2}} + \sum_{j=4}^{9} K_j \overline{Y}^{j-4}\,, \quad (1.42)$$

with

$$K_0 := \frac{c_{17}}{2} + \frac{1}{32}\left(\frac{49c_4}{2} + \frac{17c_5}{\sqrt{2}}\right) - \frac{1}{16}\left(5G_0 + \frac{17}{2\sqrt{2}}G_1 + \frac{49}{4}G_2\right)\lambda_2 - \frac{1}{16}\left(\frac{17c_4}{2\sqrt{2}} + 5c_5\right)\lambda_3 - \frac{5\lambda_5 c_1}{16}\,,$$

$$K_1 := \frac{1}{16}\left(\frac{17c_4}{\sqrt{2}} + 5c_5\right) - \frac{1}{4}\left(\frac{G_0}{\sqrt{2}} + \frac{5}{4}G_1 + \frac{17}{4\sqrt{2}}G_2\right)\lambda_2 - \frac{1}{4}\left(\frac{5c_4}{4} + \frac{c_5}{\sqrt{2}}\right)\lambda_3 - \frac{\lambda_5 c_1}{4\sqrt{2}}\,,$$

$$K_2 := \frac{1}{8}\left(\frac{5c_4}{2} + \frac{c_5}{\sqrt{2}}\right) - \frac{1}{8}\left(\frac{G_1}{\sqrt{2}} + \frac{5}{2}G_2\right)\lambda_2 - \frac{\lambda_3 c_4}{8\sqrt{2}}\,,$$

$$K_3 := \frac{1}{12\sqrt{2}}(c_4 - \lambda_2 G_2)\,, \qquad K_4 := c_{15}\,, \qquad K_5 := c_{16}\,,$$

$$K_6 := \frac{1}{4}(c_7 - \lambda_3 c_6) - \frac{1}{4}\left(G_3 + G_5 - \frac{\lambda_3 c_2}{4}\right)\lambda_2 - \frac{\lambda_5 c_2}{4}\,,$$

$$K_7 := \frac{c_6}{12} - \frac{1}{4}\left(G_6 + \frac{1}{3}G_4 + \frac{c_2}{4}\right)\lambda_2 - \frac{\lambda_3 c_7}{12}\,, \qquad K_8 := \frac{1}{24}(c_7 - \lambda_2 G_5) + \frac{\lambda_2\lambda_3 c_2}{96}\,,$$

$$K_9 := -\frac{1}{40}\left(G_6 + \frac{c_2}{4}\right)\lambda_2\,.$$

There are three new arbitrary constants introduced in the above solution, c_{15}, c_{16}, $c_{17} \in \mathbb{R}$; with the help of the boundary conditions (1.3b) and (1.3c) one can express the last two in terms of c_{15}.

A comparison between (1.17) and (1.19), shows that the matching conditions between the inner and outer solutions at $\mathcal{O}(\delta^{5/3})$ require

$$K_4 = \Pi_{50}\,, \quad K_5 = \frac{\Pi_{41}}{\sqrt[3]{2}}\,, \quad K_6 = \frac{\Pi_{32}}{2\sqrt[3]{4}}\,, \quad K_7 = \frac{\Pi_{23}}{12}\,, \quad K_8 = \frac{\Pi_{14}}{48\sqrt[3]{2}}\,, \quad K_9 = \frac{\Pi_{05}}{240\sqrt[3]{4}}\,.$$

Routine manipulations confirm that the last four of these are identically satisfied, while the first two can be combined in conjunction with the aforementioned relationship between c_{16} and c_{15} to give a linear equation for the determination of λ_6,

$$-\frac{\nu^2\sqrt{2}\Pi_{50}}{(2-\nu)^2} - \frac{2\sqrt{2}\lambda_5 c_2}{(\nu-2)^3} + \frac{\mathcal{P}_{16}}{(\nu-2)} + \frac{\mathcal{Q}_{16}}{(\nu-2)^2} + \mathcal{S}_{16} = \frac{\Pi_{41}}{\sqrt[3]{2}}\,,$$

where

$$\mathcal{S}_{16} := \frac{1}{32}\left(4\sqrt{2}G_0 + 10G_1 + 17\sqrt{2}G_2\right)\lambda_2 + \frac{1}{16}\left(5c_4 + 2\sqrt{2}c_5\right)\lambda_3 - \frac{1}{32}\left(17\sqrt{2}c_4 + 10c_5 + 4\sqrt{2}\lambda_5 c_2\right)\,,$$

$$\mathcal{Q}_{16} := \left[\sqrt{2}G_0 + 2G_1 + \sqrt{2}(3G_2 - G_3 - G_5) + \frac{\lambda_3 c_2}{2\sqrt{2}}\right]\lambda_2 + \left[2c_4 + \sqrt{2}(c_5 - c_6)\right]\lambda_3 - 3\sqrt{2}c_4 - 2c_5 + \sqrt{2}c_7 - \frac{9\lambda_5 c_2}{\sqrt{2}}\,,$$

$$\mathcal{P}_{16} := \frac{1}{16}\left\{\left[20\sqrt{2}G_0 + 34G_1 + 49\sqrt{2}G_2 - \frac{16}{\sqrt{2}}(G_3 + G_5) + 8(G_4 + 3G_6)\right] + 2(3 + \sqrt{2}\lambda_3)c_2\right\}\lambda_2 + \frac{1}{8}\left(17c_4 + 10\sqrt{2}c_5 - 4\sqrt{2}c_6 + 4c_7\right)\lambda_3 + \frac{1}{16}\left(8\sqrt{2}c_7 - 8c_6 - 34c_5 - 49\sqrt{2}c_4 - 32\sqrt{2}\lambda_5 c_2\right)\,.$$

This completes the derivation of the six-term asymptotic approximation for the critical eigenvalue of the boundary-value problem (1.3). In the next section we examine some of the features of this result, with particular reference to [2].

1.3 Numerical results & discussion

The key outcome of the analysis carried out in the previous two sections can be summarised by the following formula

$$\lambda = \underline{\lambda_0 + \lambda_2\delta^{2/3} + \lambda_3\delta} + \lambda_4\delta^{4/3} + \lambda_5\delta^{5/3} + \lambda_6\delta^2 + \mathcal{O}(\delta^{7/3}) \qquad \text{for} \quad 0 < \delta \ll 1\,, \tag{1.43}$$

where the coefficients λ_j $(j = 0, 1, \ldots, 6)$ are calculated as discussed in the previous section. This expression captures the approximation of the smallest eigenvalue of the boundary-value problem (1.3) as a function of δ. Except for λ_0, the remaining λ_j's in our result above are independent of η. However, the terms with $j \geq 3$ depend on Poisson's ratio ν. It is therefore instructive to investigate how these coefficients vary with ν; Figure 1 sheds some light on this aspect for the newly calculated λ_j's $(j = 4, 5, 6)$. We draw attention to the fact that both λ_4 and λ_6 are positive for all admissible values of ν, but λ_5 is negative. The important implications of this feature for the above asymptotic approximation will be elucidated next.

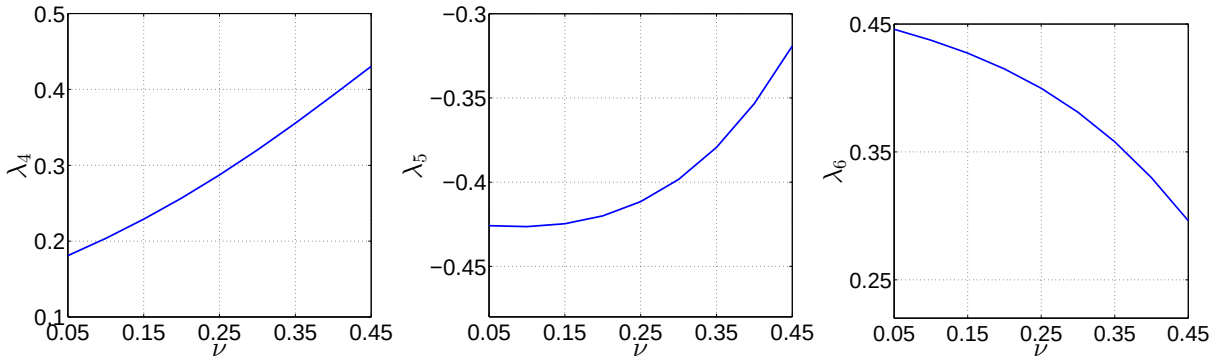

Figure 1: Variation of the newly calculated coefficients λ_j $(j = 4, 5, 6)$ from the asymptotic expansion (1.43) on Poisson's ratio ν, for $0.05 \leq \nu \leq 0.45$.

The accuracy of formula (1.43) is illustrated in Figure 2, where $\eta = 4.1$ and three values of Poisson's ratio ν are considered. We have intentionally included instances of the asymptotic parameter δ that, strictly speaking, are not particularly small. The information in this Figure suggests that the accuracy of (1.43) increases as ν decreases. As already pointed out earlier, the three-term truncation of this asymptotic formula (i.e., the underlined part) provides a slightly better accuracy since the net contribution of the last three terms is a positive quantity (while the lowest spectral value λ predicted by the full numerical simulations of (1.3) is actually negative for all values of $0 < \nu < 0.5$). For the sake of brevity we do not include additional plots as the differences mentioned are only marginally different from the ones already shown.

Another point to consider concerns the accuracy of the asymptotic approximation of λ with respect to the *number of terms* retained in formula (1.43). Figures 3 and 4 present two examples that highlight this issue. The round markers seen there represent the values provided by the six different truncations possible; these are joined sequentially by continuous lines to facilitate the zig-zag nature of the pattern followed by those points. Because the newly calculated coefficients λ_j alternate in sign, the conclusion that emerges from our numerical experiments is that, for fixed δ, simply including more terms does not necessarily ensure better outcomes. In fact, the data shown in the aforementioned figures, along with other similar numerical simulations (not included here for brevity reasons), suggests that retaining only the first three terms from (1.43) yields the best results; in this sense, the asymptotic work reported in

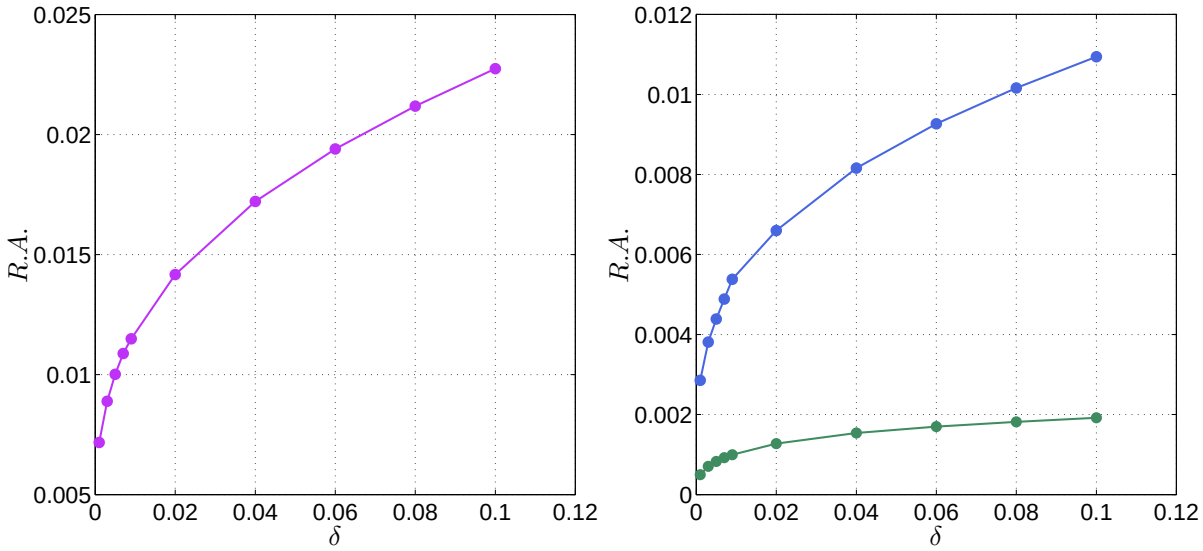

Figure 2: Relative accuracy ($R.A.$) of the asymptotic result (1.43) for $\nu = 0.4$ (left window) together with $\nu = 0.30$ and $\nu = 0.15$ (right window); the last two values correspond to the *blue* and *green* curves, respectively. In each window the circular markers are associated with $\delta = 0.1, 0.08, 0.06, \ldots, 0.003, 0.001$, while linear interpolation between them was used to emphasise the global trend of the computed relative errors; $\eta = 4.1$ in both windows.

[2] is optimal. This finding is not completely unexpected since we are working with an *asymptotic* series rather than a *convergent* one (recall the discussion in §1). For a fixed number of terms, the accuracy of the approximation does improve as δ decreases. However, increasing the number of terms in the asymptotic expansion while keeping this asymptotic parameter constant may not lead to enhanced predictions.

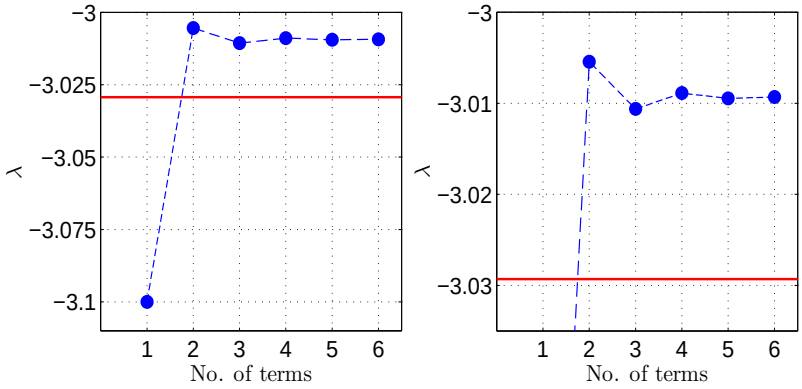

Figure 3: The effect of various truncations of the asymptotic approximation (1.43) for $\eta = 4.1$, $\nu = 0.3$, and $\delta = 0.02$. The horizontal red line corresponds to the value of λ obtained from the full numerical solution of the eigen-problem (1.3), while the window on the right provides a zoomed-in view of the plot on the left.

A final aspect that merits further elaboration is the role of the parameter η in the original boundary-value problem (1.1)-(1.2); it is this particular parameter that reflects the most serious shortcomings

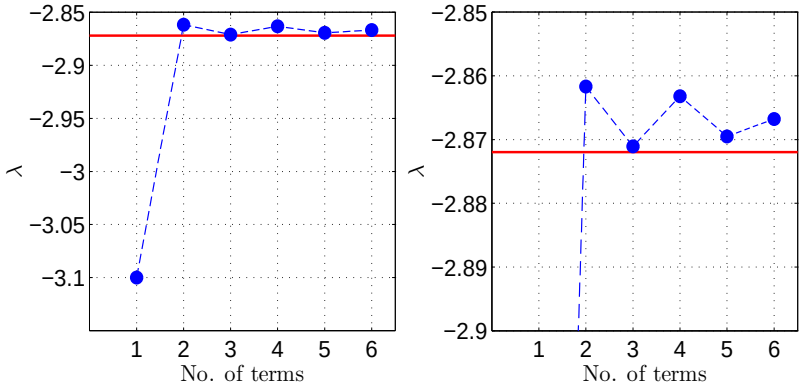

Figure 4: The same as per Fig. 3, except that here $\nu = 0.15$, and $\delta = 0.08$.

of formula (1.43). The previous study [2] was based on that particular form, whereas the present investigation adopts the re-scaled version (1.3), in which a new asymptotic parameter, $\delta \equiv \eta\beta$, was introduced (see §1). This re-formulation is more natural and offers a significant advantage by simplifying the asymptotic analysis (cf. [2]). However, it is important to note that η still influences the buckling problem, albeit indirectly – through its appearance in the endpoints of the domain on which the differential equation (1.3a) is defined. The implication is that, for fixed $0 < \delta \ll 1$, increasing η causes the solutions of the bifurcation problem (1.3) to become progressively localised near the edge of the web. This behaviour is intuitive, as increasing η while keeping δ fixed corresponds to decreasing β, thereby enhancing the singularly-perturbed character of the original problem (1.1)-(1.2). In the present work, this apparent increase in localisation arises directly from the expansion of the (rescaled) width of the web – represented by the interval $[1-\eta, 1+\eta]$ – rather than from any change in the exponential character of the solutions.

The convergence between the asymptotic formula (1.43) and the corresponding direct numerical simulation of the bifurcation problem is illustrated in Figure 5 for three representative values of $\eta \in \{2.1, 3.1, 4.1\}$. Only the underlined part in (1.43) was used, as the full six-term approximation is, to the level of visual inspection, virtually indistinguishable from the plotted curves. In each window, the asymptotic result is shown as a dashed curve, while the solid curve represents the numerical solution. The latter approach the horizontal asymptotes $\lambda = \lambda_0 \equiv 1 - \eta$, with the asymptotic curves closely replicating this behaviour. Since the approximation developed in this work involves fractional powers of δ (specifically, one-third powers), the convergence is relatively slow and may appear visually similar across all three examples shown in Figure 5. This aspect is further clarified in Figure 6, which confirms that the relative errors between the asymptotic and numerical results actually decrease as η increases away from $\eta = 1$. These differences may stem from the fact that the absolute value of the leading term λ_0 in (1.43) increases with η. As already noted at the start of this section, the coefficients λ_j ($j \geq 1$) in (1.43) are independent of η; one of the implications of this observation is that the dashed curves in Figure 5 are obtained by vertically shifting the "master curve" $\delta^{-1} \mapsto \lambda_2\delta^{2/3} + \lambda_3\delta$ by an amount equal to λ_0.

As noted at the beginning of §1.1, the validity of the asymptotic ansatz for λ in equation (1.5) relies on the ordering $|\lambda_0| \gg |\lambda_2\delta^{3/2}| \gg |\lambda_3\delta| \gg \ldots$; since λ_0 is the only coefficient that depends on η, this ordering may break down as $\eta \to 1^+$, potentially violating the leading inequality. However, the remainder of the hierarchy remains unaffected by this and continues to hold in that limit. Numerical experiments indicate that the asymptotic formula (1.43) retains its validity (and good accuracy), at

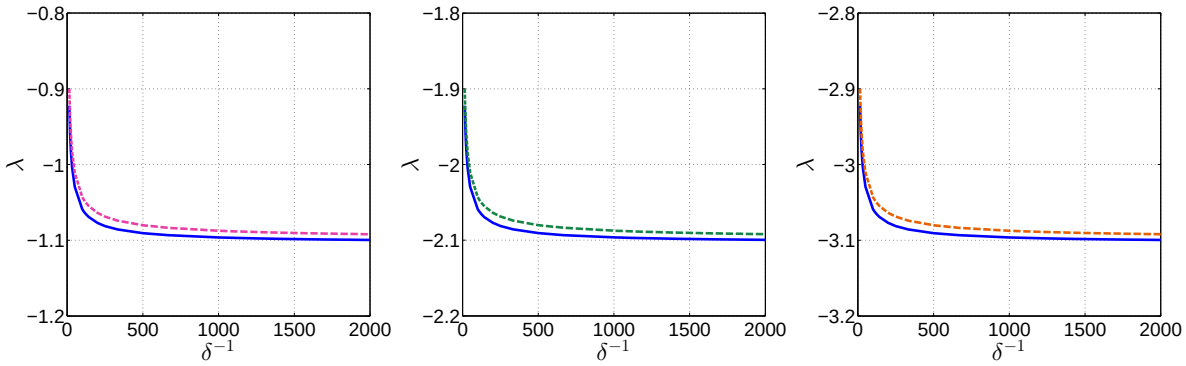

Figure 5: Convergence of the three-term (optimal) asymptotic approximation derived from (1.43) as $\delta^{-1} \to +\infty$. The three windows correspond to $\eta = 2.1$ (left), $\eta = 3.1$ (middle), and $\eta = 4.1$ (right). In each case the solid blue curve represents the numerical solution of the boundary-value problem (1.3), while the dashed curve depicts the corresponding asymptotic approximation. Here $\nu = 0.3$ and $5 \times 10^{-4} \leq \delta \leq 7 \times 10^{-2}$.

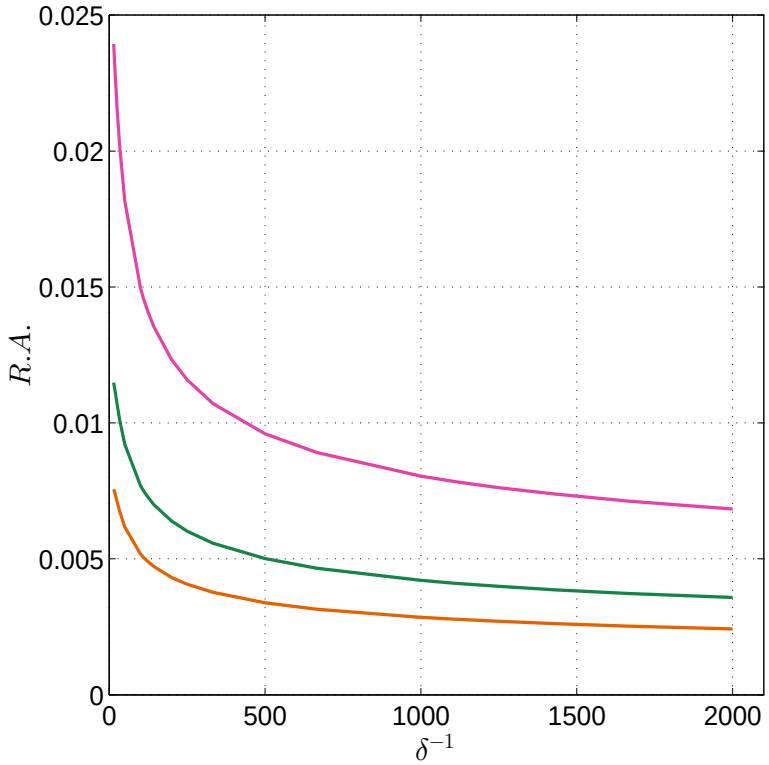

Figure 6: Relative accuracy (*R.A.*) associated with the three parameter values considered in Fig. 5; the curves correspond, from top to bottom, to $\eta = 2.1$, 3.1, and 4.1.

least for small ν-values. In Figure 7 we illustrate the convergence of our three-term approximation for $\eta = 1$ and $\eta = 2.1$ in the case $\nu = 0.15$.

Although the *global* errors in both plots shown in Figure 7 are excellent, the relative accuracies tell a different story, as illustrated in Figure 8. In the case $\eta = 1$, the approximation progressively loses

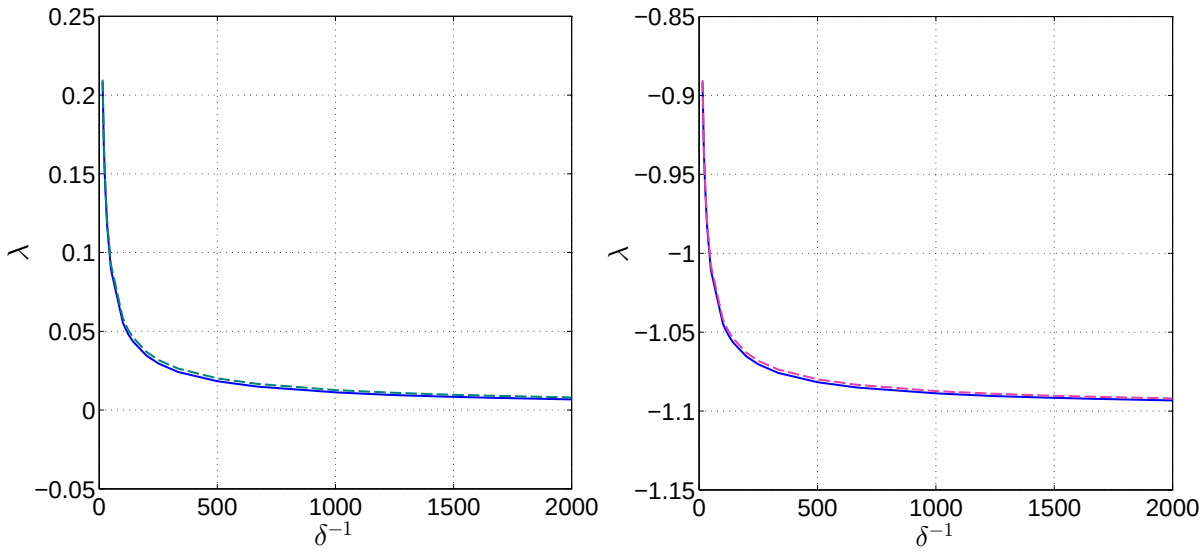

Figure 7: Convergence of the three-term approximation obtained from (1.43) for $\eta = 1$ (left) and $\eta = 2.1$ (right). In both windows $\nu = 0.15$.

accuracy as $\delta \to 0^+$. As discussed at the beginning of §1.1, the asymptotic analysis was developed under the assumption that $0 < |1 - \eta| = \mathcal{O}(1)$. When $\eta = 1$, this assumption breaks down, the asymptotic ansatz (1.5) becomes ill-posed, and there is no reason to expect the validity of the analysis presented here. Furthermore, the divergence of the relative errors observed in the left window of

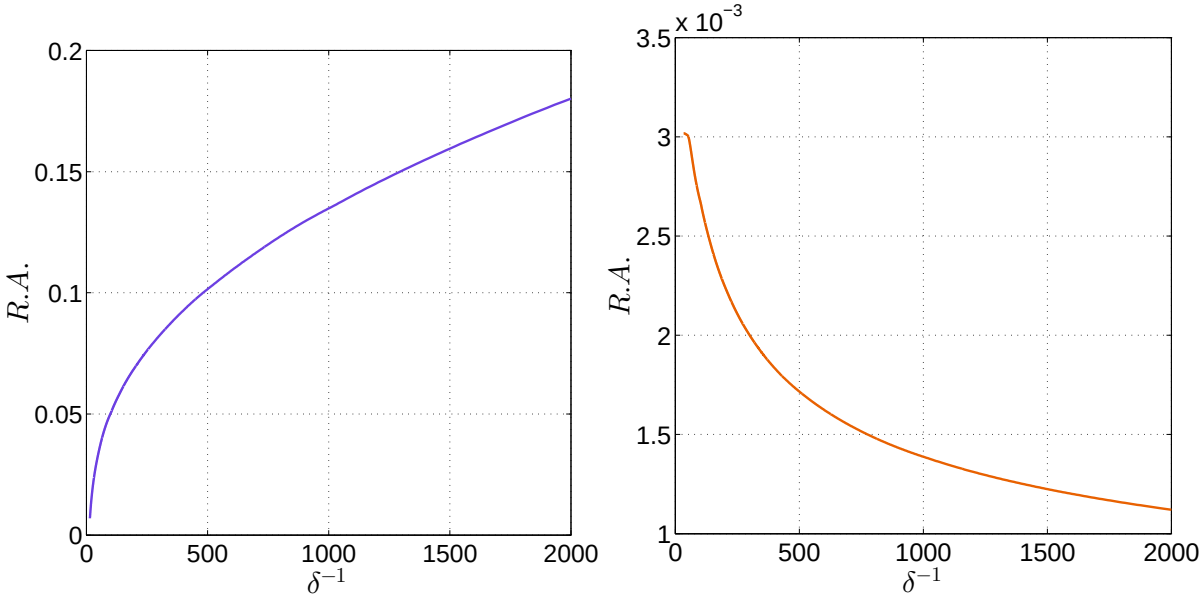

Figure 8: Relative accuracies for the two sets of comparisons in Fig. 7; $\eta = 1$ (left) and $\eta = 2.1$ (right).

Figure 8 is not incidental, although the severity of this effect appears to become more pronounced as the Poisson's ratio increases.

In conclusion, the asymptotic analysis above demonstrates that the tentative approximation of the

critical eigenvalue of the BVP (1.3), as proposed in [2], provides reasonably good accuracy when η is not too close to unity and δ is only moderately small. However, this approximation breaks down in the limit $\eta \simeq 1$. As demonstrated in BC25, one reason for this discrepancy is that, in this regime, the critical eigenmode is no longer governed by Airy-type functions but instead by a simple linear combination of pure exponentials – qualitatively identical to the case $\eta = 0$ previously analysed by the first author in the same reference. In light of this observation, the asymptotic formula (1.43), while generally accurate, does not fully capture the true asymptotic behavior of $\lambda(\delta)$ as $\delta \to 0^+$. In this respect, the present approximation is reminiscent of those derived via Rayleigh's quotient, where the use of an approximate test function can yield highly accurate eigenvalue estimates, even when the corresponding eigenmodes are not accurately reproduced [5, 6].

References

[1] Coman, C.D., Bassom, A.P.: Remarks on boundary layers and matched asymptotics for an edge-buckling problem. (Submitted to Journal of Mechanics of Materials and Structures, 2025)

[2] Coman, C.D.: Divergence instabilities of non-uniformly pre-stressed travelling webs. Journal of Mechanics of Materials and Structures **19**, 109–130 (2024)

[3] Coman, C.D.: A WKB approximation for the divergence-buckling of a travelling web. Acta Mechanica **236**, 3873–2892 (2025)

[4] Coman, C.D.: Instabilities of highly anisotropic spinning disks. Mathematics and Mechanics of Solids **16**, 3–17 (2011)

[5] Temple, G., Bickley, W.G.: Rayleigh's Principle and Its Applications to Engineering. Dover Publications, New York (1956)

[6] Kantorovich, L.V., Krylov, V.I.: Approximate Methods of Higher Analysis. P. Noordhoff, Groningen (1958)